Service Life Extension and Maintenance Optimization of Electromechanical Components

Robby Christian [a], Hyun Gook Kang [b*]
[a,b]*KAIST, Nuclear & Quantum Eng. Dept., 291 Daehak-ro, Yuseong-gu, Daejeon 305-701*
[*]*Corresponding author: hyungook@kaist.ac.kr*

1. Introduction

Electromechanical components are commonly used in nuclear power plants and other nuclear installations. Because they have moving parts, their wear and tear is usually more severe than static components. For that reason, they require a more stringent inspection and maintenance program to prevent failures from occurring. However, these programs themselves may induce faults on the component such that performing frequent inspection services is not always desirable [1]. The Condition Based Maintenance (CBM) approach has gained recognition for resolving this issue.

The CBM attempts to perform maintenance only when it is required as suggested by the component's latest condition. This method implies the need for additional monitoring instrumentation costs. Furthermore, the CBM may require sudden, unplanned maintenance events and therefore the availability of a maintenance team at any time. This may be more costly compared to fixed maintenance schedules because it requires the maintenance team and equipment to be always available at any time.

This paper proposes an integrated method to optimize the CBM by using prognostics methodology to manage the operation of an electromechanical component. The optimization is expected to prolong the component's service life and minimize CBM costs.

2. Methods

2.1. Model Predictive Controller

The approach we propose to extend the service life of an electromechanical component is through the use of a dynamic controller which can adjust its output based on the component's degradation state. In this study we selected a Model Predictive Controller for this purpose. The working principle of an MPC is shown in Fig 1. A model of the component is continuously updated as a part of an online monitoring program. Degradations in the component is then reflected in the change of model parameters. Output of the MPC is adjusted based on this model information to maintain the desired performance of the component. This is done by minimizing a cost function as given in equation (1).

$$J = \sum_{k=1}^{p} s(k) - m(k)\,, \qquad J \geq 0 \qquad (1)$$

Where s(k) is the target setpoint value covering the transient response characteristics i.e. rise time, maximum overshoot and steady state error, while m(k) is the model's output. We omitted the squared error formulation to give leeway for the second optimization discussed later in this paper.

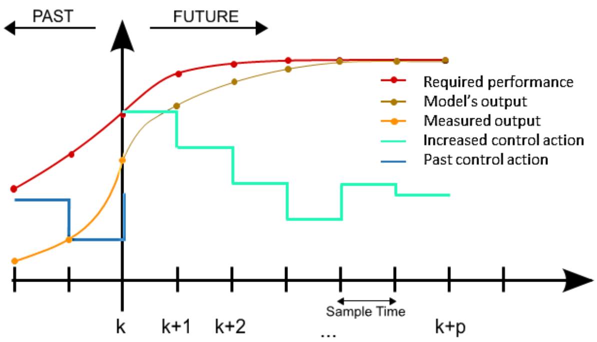

Fig. 1. Working principle of an MPC

The MPC has a finite range of control actions. Beyond a certain level of degradation, the MPC will not be able to exert enough control to maintain the component's performance. This level defines the point of failure as illustrated in Fig 2.

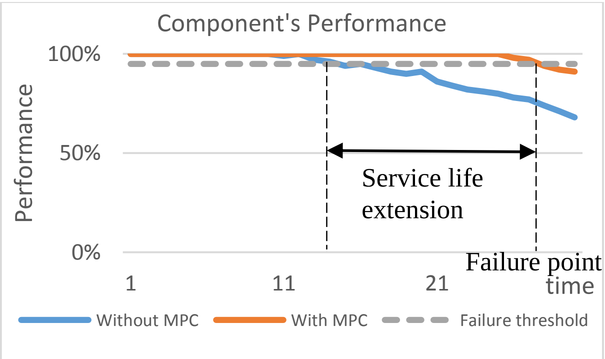

Fig. 2. Component's extension of useful life due to MPC

2.2. Fault Growth Modelling and Failure Prediction

The underlying principle for fault growth was adopted from the Eyring model which is based in quantum mechanics principles [2]. It recalls that environmental stresses generate the activation energy needed to cross an energy barrier in the quantum level to initiate a reaction which creates physical fault such as crack, deformation or oxidation. In this research setting, the environmental stress *v(k)* was characterized into deterministic and stochastic stresses as follows:

$$v(k) = \rho(k).\omega(k) + \mu(k).\omega(k) \qquad (2)$$

where $\omega(k)$ is the stochastic environmental condition which inflict stresses upon the actuator system while $\rho(k)$ and $\mu(k)$ are the deterministic correcting factor to

$\omega(k)$ which determine the extent of the stress exerted on the component. $\rho(k)$ increases stress due to a more stringent control actions when faults are present. In contrast, $\mu(k)$ reduces it when the component, or parts of the component, is not operating or in standby mode. By these definitions, $0 \leq \mu(k) \leq 1$ and $\rho(k) \geq 1$ for mechanically moving parts, while $\rho(k) = 0$ and $\mu(k) = 1$. These factors can be measured by comparing degradation states between different operating states. The difference of these correction factors is shown in Fig 3.

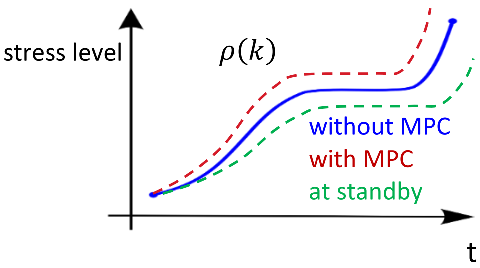

Fig. 3. Stress level as a function of component's operational state

The stochastic environmental condition $\omega(k)$ is further classified into bounded and unbounded load variations which probability functions are given in equation (3) and equation (4) respectively. The variable n in equation (4) is the number of discrete states of ω. Bounded ω comes from the variation of environmental condition where the component is installed, i.e. temperature, pressure, humidity. Unbounded ω originates from freely-oscillating stressors with a uniform distribution over their normalized discrete states n. Several examples of stressors which fall into this category are the component's operation profile, demanded load, and electronic disturbances.

$$Pr(\omega(k) = \omega) = Pr(\omega(k) = \omega|\omega(k-1) = v), v\epsilon W \quad (3)$$

$$Pr(\omega(k) = \omega) = \frac{1}{n} \quad (4)$$

The type of environmental variations affecting the component depends largely on the component's design itself and installation conditions. For example, internal parts such as a motor's armature may be insulated thereby allowing only unbounded stress variations to affect fault growths in it. In this study we focus on the faults which are irreversible throughout the component's operation and are fixed during the maintenance process. The relationship between environmental condition and fault growth is illustrated in Fig 4. This kind of faults satisfies a monotonically increasing function up to the maintenance period as follows:

$$\forall\, t \leq t_{maintenance}: fault_{t+1} \geq fault_t \quad (5)$$

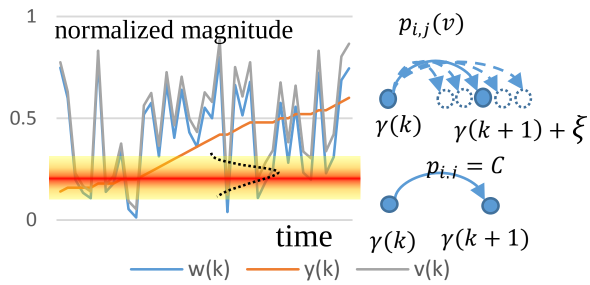

Fig 4. Monotonic fault growth $\gamma(k)$ as a function of environment and control loads

From the abovementioned analysis, the fault evolution was modelled as a second order Markov Chain process as follows [3]:

$$p_{i,j}(v) = \Pr(\gamma(k+1) = s_j | \gamma(k) = s_i, v(k) = v),$$
$$\gamma, s_i, s_j \in S, \quad v \in V(k), \quad k \in \mathbb{N} \quad (6)$$

$$\sum_{s_j \in S} p_{i,j} = 1 \quad (7)$$

where

$p_{i,j}(v)$: probability of transitioning from one DS s_i to s_j given an applied load v

γ : random variable representing component's DS

S : state space for component's DS

V(k) : domain of feasible loads that may be applied at a given time-instant

It is expected that there are aleatoric uncertainties in the predicted damage level should a load above its minimum energy barrier is imposed. This uncertainty is incorporated in the model by introducing a noise term ξ in the Markov Chain model as shown in Fig 5, which is a similar practice to the reference studies [4],[5]. In contrast, the damage level is expected to remain the same when the load is below the minimum energy barrier. However in order to accommodate incipient faults and epistemic uncertainties in the fault growth physics, an arbitrarily small probability value C was additionally introduced which may lead to an increase in the Degradation State (DS). For this reason, the fault evolution mechanism was then mathematically expressed as follows:

$$p_{i,j}(\rho)|\omega \geq \beta = \sum_{\omega\epsilon W} \sum_{\xi\epsilon\Xi} Pr(\omega(k) = \omega) \,.\, Pr(\xi(k) = \xi) \,.\, Pr\,(\beta = \beta_{true}) \quad (8)$$

$$p_{i,j}(\rho)|\omega < \beta = C.Pr(\beta = \beta_{true}) \doteq C \ll 1 \quad (9)$$

where W and Ξ are the state spaces for ω and ξ respectively, while β is the normalized minimum energy barrier zone.

Since failure is measured in terms of the MPC's capability to maintain the system's performance, it is desirable to map the relation between the internal degradation state and the controller's capability to compensate it. This fault compensation capability is reflected by the term Adaptive Space (AS). Thus AS has a value of 100% when the system is healthy, and 0% when the system fails. The objective of this prognostics module is therefore to continuously predict when AS' value will reduce to 0. However it was not hypothesized as a straightforward task. The component's model which serve as the basis of MPC may contain inaccuracies from model simplification, sensor errors and various noise signals. As a consequence, the variable AS as a function of DS is expected to be noisy. Furthermore, the variance of AS is inversely proportional to the DS due to an increasing Signal-to-Noise (SNR) profile. This phenomena where DS, a stochastic state satisfying the Markov property, generates AS, another stochastic variable of observational interest, can be conveniently portrayed as a Hidden Markov Model (HMM) shown in Fig 5. The DS transition probability $p_{i,j}$ was given in equation (20) and equation (21) where $\sum_{s_j \in S} p_{i,j} = 1$. The observed AS probability distribution $q_{k,l}$ was determined by experiment where $\sum_{\zeta(l)\in Y} q_{k,l} = 1$.

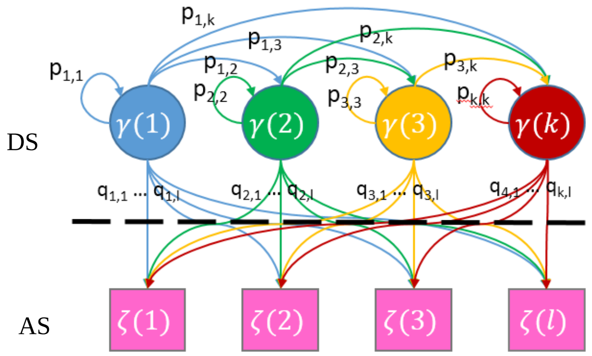

Fig 5. Hidden Markov Model (HMM) structure revealing the monotonic fault progression and its relationship with the controller's adaptiveness

The HMM parameters $p_{i,j}$ and $q_{k,l}$ can be obtained through experiments by monitoring the environmental conditions and measuring the component's damage growth per failure mode. This experiment should be done several times with different component specimens to obtain the aleatoric uncertainty profile which is determined by the variations in the component's manufacturing process.

After the HMM's parameters are identified, the HMM model serves as a prior likelihood of fault evolution for the component's type. However due to variations in manufacturing process, transportation and installation, each component specimen has a slightly different fault mode and progression. In order to properly predict a component's fault characteristics, the Bayesian inference method is used to form the posterior likelihood of DS $\gamma(t)$ using the HMM as a prior and the calculated AS $\zeta(t)$ of the specific component. A particle filter algorithm is then employed on this likelihood to estimate $Pr(\gamma(t+k))$, $Pr(\zeta(t+k))$ and the $Pr(t|\zeta_1)$.

The prediction of future AS probabilities $Pr(\zeta(t+k))$ is shown in Fig 6. A vertical cut of this figure gives information on the risk profile of the component given a specific mission time. For example, the probability of AS ≤ 0 at time t_3 is as follows:

$$P_{t_3} = \int_{-\sim}^{0} Pr(\zeta|t=t_3)d\zeta = 1 - \int_0^{ASmax} Pr(\zeta|t=t_3)d\zeta \qquad (10)$$

While the horizontal cut gives an answer on when the next maintenance should be done. The probability of component's failure before a postulated maintenance schedule t_4 is as follows:

$$Pr_{fail} = \int_0^{t_4} Pr_{RUL}(t|\zeta=0)dt \qquad (11)$$

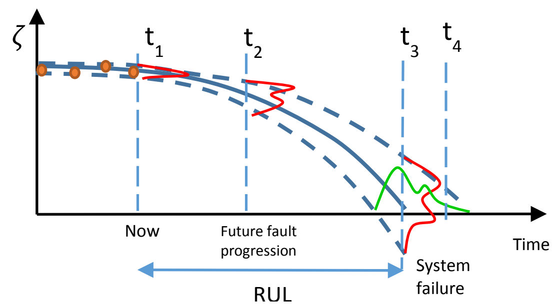

Fig. 6. Probabilistic prediction of future AS

2.3. Maintenance Optimization

It is recognized that in a system, CBM may co-exist with a conventional Planned Scheduled Maintenance (PM) program. This is because a PSM program may be more suitable for some components over a CBM one. The objective of this optimization as shown in Fig 7 is then to reduce the system's downtime in a combined maintenance program while at the same time keeping the system's prime performance. By attempting to coincide the CBM with PM, the maintenance costs can also be reduced.

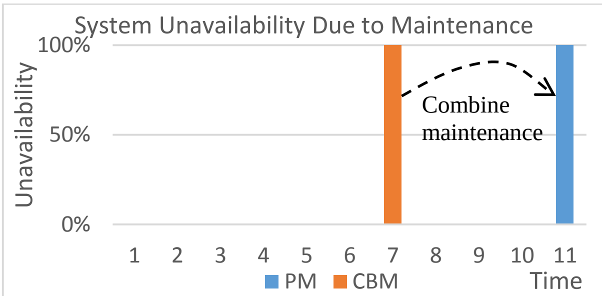

Fig. 7. System unavailability and optimization objective

Having the aforementioned optimization objective, its loss function can be written as follows:

$$J = \min_{\zeta(l)\in Y} w_1 \sum_{k=1}^{p} s(k) - m(k) + w_2 Pr(t_{RUL} = t_{PM}|\zeta(l)), \quad J \geq 0 \qquad (12)$$

Where w_1 and w_2 are weighting factors indicating the degree of priority of the optimization program.

2.4. Application of methodology

The methodology was applied on the anode voltage regulator system of an ion implantation accelerator which schematic is given in Fig 8. The regulator system is composed of a DC motor actuator driven by an H-bridge chopper driver with a Pulse Width Modulation (PWM) switching signal. It controls the operating voltage of a motor-generator which generates the anode voltage. The regulator fails when it has a slow rise time and settling time, high steady state error and overshoot.

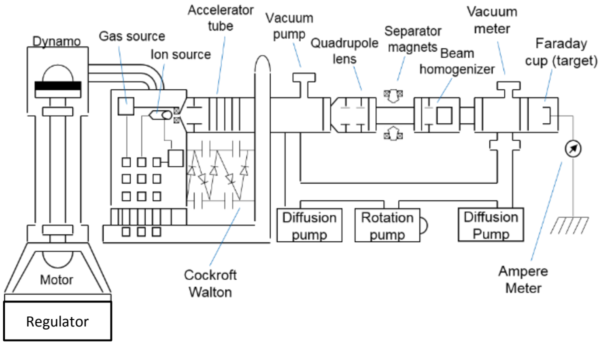

Fig. 8. Schematic of ion implantation accelerator

3. Results

The optimization process is shown in Fig 9. It shows the estimate of future adaptive state predicted at the initial and late stage of the system's degradation. The target of the optimization is to maintain system's performance despite of degradation for an additional 514 operation cycles when a routine maintenance is scheduled.

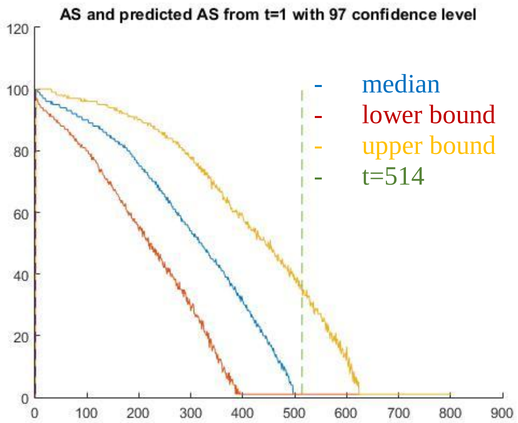

(a) Estimated AS and failure time at the early stage of degradation

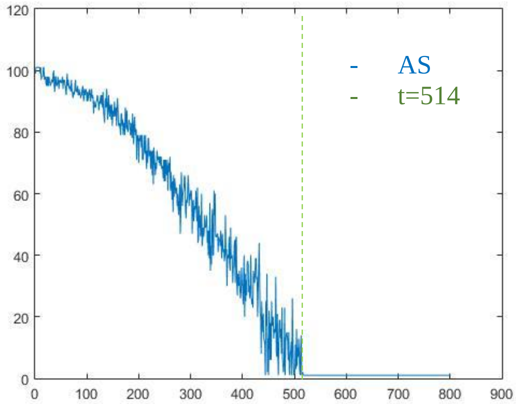

(b) AS and failure time at the final stage of degradation

Fig. 9. Optimization of controller actions AS

Fig 10 shows the comparison of performance between when this optimization methodology is applied and when it is not. The comparison is made from when degradation was first observed. Although the steady-state error of the unoptimized system started to exceed its threshold at t+348, the rise time and settling time had already deviated earlier at t=1. Therefore in this case the unoptimized system failed at t=1. Increasing the controller's action inevitably increased the system's maximum overshoot, however it is still below the prescribed threshold of 1%. The figures showed that the system's performance was successfully maintained until t=514.

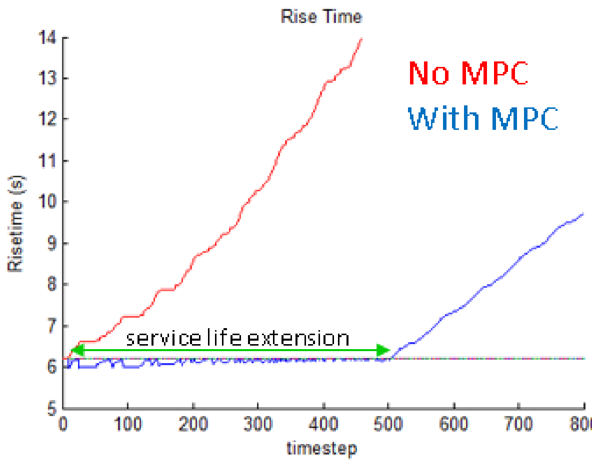

(a) Comparison of rise time

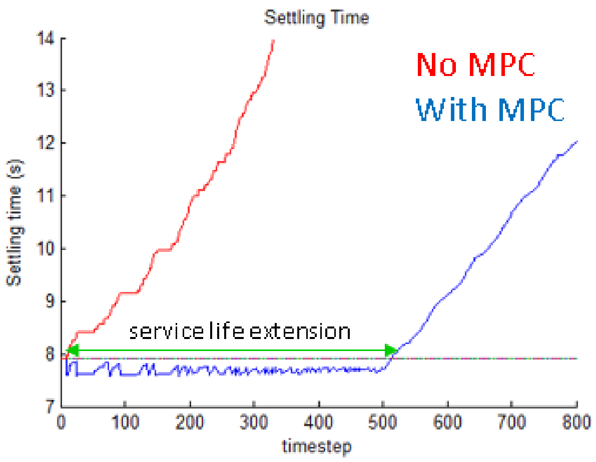

(b) Comparison of settling time

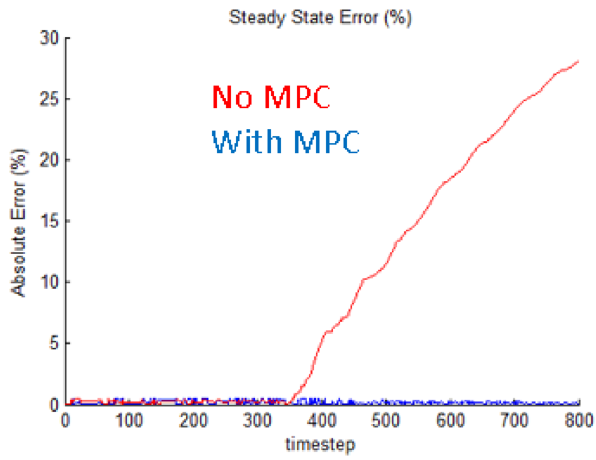

(c) Comparison of steady-state error

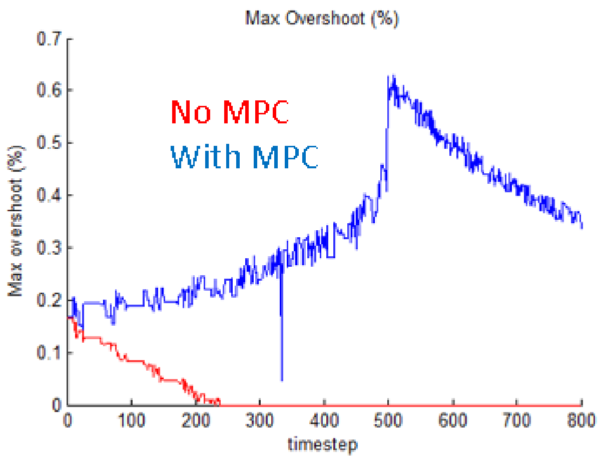

(d) Comparison of maximum overshoot

Fig. 10. Performance comparison when optimization was applied

4. Conclusions

A fault growth model was presented taking into account aleatoric and epistemic uncertainties. This model was coupled with an MPC to preserve the degrading component's performance within desired specification. The controller's actions were further optimized to coincide the under-performance-time with the planned maintenance schedule. This approach may reduce maintenance labor's costs and system unavailability. Experiment results confirmed that the proposed methodology successfully meet its designated objectives.

REFERENCES

[1] S.M. Shin, I.S. Jeon, H.G. Kang, Surveillance Test and Monitoring Strategy for the Availability Improvement of Standby Equipment Using Age-Dependent Model, Reliab. Eng. Syst. Saf., Vol. 135, pp. 100-106, 2015.

[2] A. Saxena, K. Goebel, D.Simon, Damage Propagation Modeling for Aircraft Engine Run-to-Failure Simulation, Proceedings of the 2008 International Conference on Prognostics and Health Management, Denver, 2008.

[3] B.M. Bole, K. Goebel, G. Vachtsevanos, Using Markov Models of Fault Growth Physics and Environmental Stresses to Optimize Control Actions, Proceedings of Infotech@Aerospace, California, 2012.

[4] B. Saha, K. Goebel, Uncertainty Management for Diagnostics and Prognostics of Batteries Using Bayesian Techniques, Proceedings of IEEE Aerospace Conference, California, 2008.

[5] M. Orchard, G. Kacprzynski, K. Goebel, B. Saha, G. Vachtsevanos, Advances in Uncertainty Representation and Management for Particle Filtering Applied to Prognostics, Proceedings of the 2008 International Conference on Prognostics and Health Management, Denver, 2008